JBC ARTICLE

The lysosomal Ca^{2+} release channel TRPML1 regulates lysosome size by activating calmodulin

Received for publication, December 12, 2016, and in revised form, March 29, 2017 Published, Papers in Press, March 30, 2017, DOI 10.1074/jbc.M116.772160

Qi Cao[1], **Yiming Yang**[1], **Xi Zoë Zhong, and Xian-Ping Dong**[2]

From the Department of Physiology and Biophysics, Dalhousie University, Halifax, Nova Scotia B3H 4R2, Canada

Edited by Roger J. Colbran

Intracellular lysosomal membrane trafficking, including fusion and fission, is crucial for cellular homeostasis and normal cell function. Both fusion and fission of lysosomal membrane are accompanied by lysosomal Ca^{2+} release. We recently have demonstrated that the lysosomal Ca^{2+} release channel P2X4 regulates lysosome fusion through a calmodulin (CaM)-dependent mechanism. However, the molecular mechanism underlying lysosome fission remains uncertain. In this study, we report that enlarged lysosomes/vacuoles induced by either vacuolin-1 or P2X4 activation are suppressed by up-regulating the lysosomal Ca^{2+} release channel transient receptor potential mucolipin 1 (TRPML1) but not the lysosomal Na^{+} release channel two-pore channel 2 (TPC2). Activation of TRPML1 facilitated the recovery of enlarged lysosomes/vacuoles. Moreover, the effects of TRPML1 on lysosome/vacuole size regulation were eliminated by Ca^{2+} chelation, suggesting a requirement for TRPML1-mediated Ca^{2+} release. We further demonstrate that the prototypical Ca^{2+} sensor CaM is required for the regulation of lysosome/vacuole size by TRPML1, suggesting that TRPML1 may promote lysosome fission by activating CaM. Given that lysosome fission is implicated in both lysosome biogenesis and reformation, our findings suggest that TRPML1 may function as a key lysosomal Ca^{2+} channel controlling both lysosome biogenesis and reformation.

Lysosomes constitutively undergo fusion and fission to accomplish their functions (1, 2). As with the synaptic vesicle fusion and fission with the plasma membrane, lysosome fusion and fission with other membranes are also Ca^{2+}-dependent (3–11). It is believed that the lysosome itself (and/or other organelles) is the major Ca^{2+} source responsible for the fusion and fission processes (7, 8). Our recent work suggested that P2X4 functions as a lysosomal Ca^{2+} channel that regulates lysosome fusion through a calmodulin (CaM)-dependent[3] mechanism (12). However, the molecular identity of the lysosomal Ca^{2+} release channel that regulates lysosomal fission remains elusive.

Transient receptor potential mucolipin 1 (TRPML1) (10, 13–15) belongs to the large family of transient receptor potential ion channels that permeates Ca^{2+}, Na^{+}, and other cations (10, 15–28). Mutations in TRPML1 gene lead to mucolipidosis type IV (ML4) disease, which is characterized with defects in membrane trafficking in the late endocytic pathway (10, 29), enlarged lysosomes (10, 29), and impaired lysosome biogenesis (30–32). Interestingly, cells deficient in phosphatidylinositol 3,5-bisphosphate (PI(3,5)P2), the lysosome-specific phosphoinositide, also exhibit trafficking defects in the late endocytic pathway and enlarged lysosomes (10, 14), and PI(3,5)P2 up-regulation promotes the fission of yeast vacuoles, the counterpart of mammalian lysosomes (33, 34). Recently, we have shown that TRPML1 is activated by PI(3,5)P2, and the enlarged vacuolar phenotype observed in PI(3,5)P2-deficient mouse fibroblasts is rescued by TRPML1 overexpression (14). These published results suggest that TRPML1 may regulate lysosome membrane fission by transducing information regarding PI(3,5)P2 levels into changes in juxtaorganellar Ca^{2+} levels.

To explore the mechanism of lysosome membrane fission, we have attempted to directly detect fission events using live imaging. Unfortunately, we failed to obtain convincing data to present. Alternatively, we used the recovery of enlarged lysosomes as a readout of membrane fission. We found that the enlargement of lysosomes induced by either vacuolin-1 or P2X4 activation was suppressed by up-regulating TRPML1. TRPML1 activation also facilitated the recovery of enlarged lysosomes. The effect of TRPML1 activation on lysosome recovery was eliminated by BAPTA-AM treatment, suggesting a requirement of Ca^{2+} release through TRPML1 for lysosome fission. We also observed that loss of TRPML1 enlarged lysosomes and suppressed enlarged lysosome recovery. Furthermore, the enlarged lysosome recovery was strongly suppressed by inhibiting the prototypical Ca^{2+} sensor CaM but not the other lysosomal Ca^{2+} sensor protein, ALG-2 (apoptosis-linked gene-2), suggesting that CaM acts as the Ca^{2+} sensor regulating

This work was supported by start-up funds (to X.-P. D.) from the Department of Physiology and Biophysics, Dalhousie University, Dalhousie Medical Research Foundation (DMRF) Equipment Grant, DMRF new investigator award, Canadian Institutes of Health Research Grant MOP-119349, Canadian Institutes of Health Research New Investigator Award 201109MSH-261462-208625, Nova Scotia Health Research Foundation (NSHRF) Establishment Grant MED-PRO-2011-7485, and Canada Foundation for Innovation (CFI) Leaders Opportunity Fund for Research Infrastructure Grant 29291. The authors declare that they have no conflicts of interest with the contents of this article.

This article contains supplemental Fig. S1.

[1] Both authors contributed equally to this work.

[2] To whom correspondence should be addressed: Dept. of Physiology and Biophysics, Dalhousie University, Sir Charles Tupper Medical Bldg., 5850 College St., Halifax, Nova Scotia B3H 4R2, Canada. Tel.: 902-494-3370; Fax: 902-494-1685; E-mail: xpdong@dal.ca.

[3] The abbreviations used are: CaM, calmodulin; BAPTA-AM, 1,2-Bis (2-aminophenoxy) ethane-*N*,*N*,*N*′,*N*′-tetraacetic acid tetrakis (acetoxymethyl ester); P2X4, P2X purinoceptor 4; TRPML, transient receptor potential mucolipin; TPC, two-pore channel; ML4, mucolipidosis type IV; PI(3,5)P2, phosphatidylinositol 3,5-bisphosphate; ML-SA, mucolipin synthetic agonist; MA, methylamine; Syt VII, synaptotagmin VII.

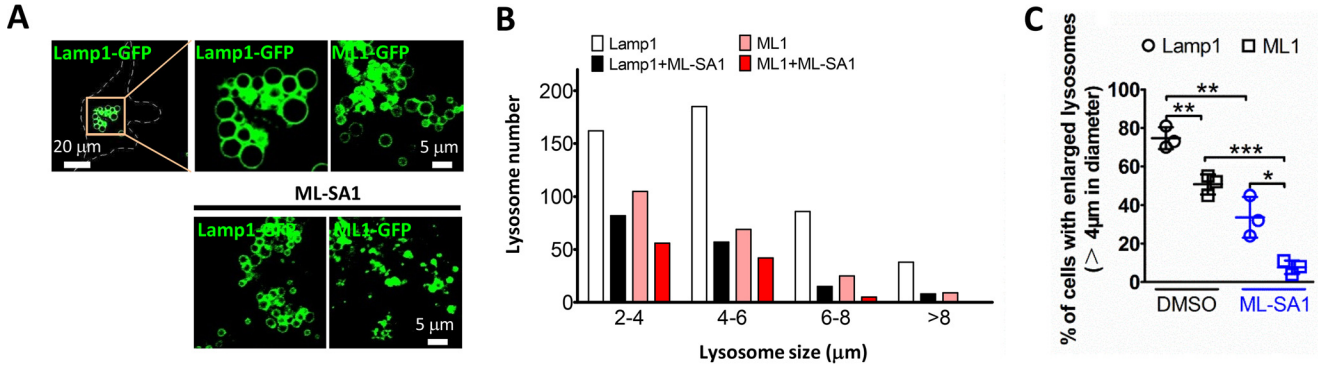

Figure 1. TRPML1 up-regulation antagonizes lysosome enlargement induced by vacuolin-1. *A*, vacuolin-1 (1 μM, 2 h) induced enlarged lysosomes that were labeled with Lamp1-GFP in Cos1 cells. TRPML1-GFP overexpression or ML-SA1 (15 μM) treatment significantly prevented vacuolin-1 from inducing lysosome enlargement. *B*, histogram for lysosome size distributions under the conditions indicated. The data were pooled from 26 cells for each condition. *C*, summary of percentage of cells containing enlarged lysosomes (at least three lysosomes of >4 μm in diameter) from three independent experiments. More than 250 cells were counted for each experiment. The experiment was repeated three times, and representative fluorescence images are shown. The cells were counted as described under "Experimental procedures." *Error bars* represent S.D. *NS*, no significance; *, $p < 0.05$; **, $p < 0.01$.

lysosomal membrane fission. Our studies suggest that TRPML1 may facilitate lysosomal membrane fission through a CaM-dependent mechanism.

Results

Activation of TRPML1 inhibits lysosome vacuolation induced by vacuolin-1

Because cells with deficiency in either TRPML1 or PI3,5P2, the endogenous TRPML1 agonist, display enlarged lysosomes (10, 14) and because PI3,5P2 has been associated with the fission of yeast vacuole, the counterpart of mammalian lysosome (29, 33, 34), we hypothesized that TRPML1 may control lysosome fission. To test this, we first treated Cos1 cells with vacuolin-1, a chemical that enlarges lysosomes (15, 35). If TRPML1 promotes lysosome fission, we expect to see smaller lysosomes in response to vacuolin-1 in cells expressing TRPML1 or treated with the TRPML1 agonist, mucolipin synthetic agonist 1 (ML-SA1, 15 μM) (17, 36). In this study, we adopted Cos1 cell as a model to study lysosome size because this cell is one of the most commonly used mammalian cell lines possessing high transfection efficiency and good morphology for imaging. Lysosome size was analyzed by counting the percentage of cells containing at least three lysosomes larger than 4 μm in diameter as described in published work (12). Indeed, TRPML1-GFP or ML-SA1 significantly reduced the lysosome size induced by vacuolin-1 (1 μM for 2 h) (Fig. 1, *A–C*). The percentage of cells containing enlarged lysosomes induced by vacuolin-1 was decreased from 74.67 ± 5.69% in cells expressing Lamp1 (lysosomal-associated membrane protein 1)-GFP to 50.67 ± 5.13% in cells expressing TRPML1-GFP. Consistently, ML-SA1 significantly decreased the percentage of Lamp1-GFP-expressing cells with enlarged lysosomes (induced by vacuolin-1) to 33.67 ± 10.60%. Co-application of TRPML1-GFP and ML-SA1 further decreased the percentage of cells with enlarged lysosomes to 7.67 ± 3.51%. These data suggest that up-regulation of TRPML1 prohibits lysosomes from enlargement.

Activation of TRPML1 promotes lysosome recovery from enlarged vacuoles

To further examine the potential role of TRPML1 in lysosome membrane fission, we enlarged lysosomes with vacuolin-1 and then evaluated the recovery of lysosome after vacuolin-1 removal. A decrease in lysosome size through time represents lysosome fission. As shown in Fig. 2 (*A* and *E*), in cells expressing Lamp1-GFP, the percentage of cells with enlarged lysosomes (>4 μm) was decreased from 72.67 ± 6.03 to 51.00 ± 1.03% after 1 h of recovery. This might be caused by endogenous TRPML1 activity. ML-SA1 (15 μM) treatment dramatically increased the recovery speed, and the percentage of cells with enlarged lysosomes was further reduced to 22.00 ± 4.31% (Fig. 2, *A*, *E*, and *F*). This recovery of lysosome size is Ca^{2+}-dependent because BAPTA-AM (10 μM), a fast and membrane-permeable Ca^{2+} chelator, remarkably inhibited the recovery (Fig. 2, *B*, *E*, and *F*).

Recombinant TRPML1-GFP also facilitated enlarged lysosome recovery after vacuolin-1 removal, compared with that of cells expressing Lamp1-GFP. The percentage of TRPML1-GFP-expressing cells with enlarged lysosomes was reduced from 56.00 ± 4.58 to 24.67 ± 2.52% with 1 h of recovery, and ML-SA1 treatment further reduced the percentage of cells with enlarged lysosomes to 4.67 ± 2.52% (Fig. 2, *C*, *E*, and *F*). The facilitation of recovery by activation of heterologous TRPML1 was also Ca^{2+}-dependent because BAPTA-AM pretreatment remarkably slowed down the recovery (Fig. 2, *D–F*). In addition, ML-SA1 promoted the recovery of enlarged lysosomes in a dose-dependent manner (Fig. 2*G*). Inversely, inhibiting TRPML1 with ML-SI1 (25 μM) (21) significantly reduced the recovery speed of enlarged lysosomes after vacuolin-1 removal (Fig. 2, *H–J*). Smaller vacuoles in cells with TRPML1 up-regulation could be attributed to increased fission or decreased fusion. Because fusion is Ca^{2+}-dependent (7, 12), it is unlikely that TRPML1-mediated Ca^{2+} release causes decreased fusion. Supporting this, loss of TRPML1 results in enlarged lysosomes (10). Altogether, our data suggest that TRPML1 may regulate lysosome fission.

Activation of TRPML1 reduces enlarged lysosomes induced by P2X4 up-regulation

Recently, we have shown that alkalization of lysosomes by methylamine (MA, 10 mM) increases the lysosome size by facilitating P2X4 activity (12). Therefore, we adopted this model to further study the role of TRPML1 in the control of lysosome size. As shown in Fig. 3*A*, enlarged lysosomes (>2 μM) induced

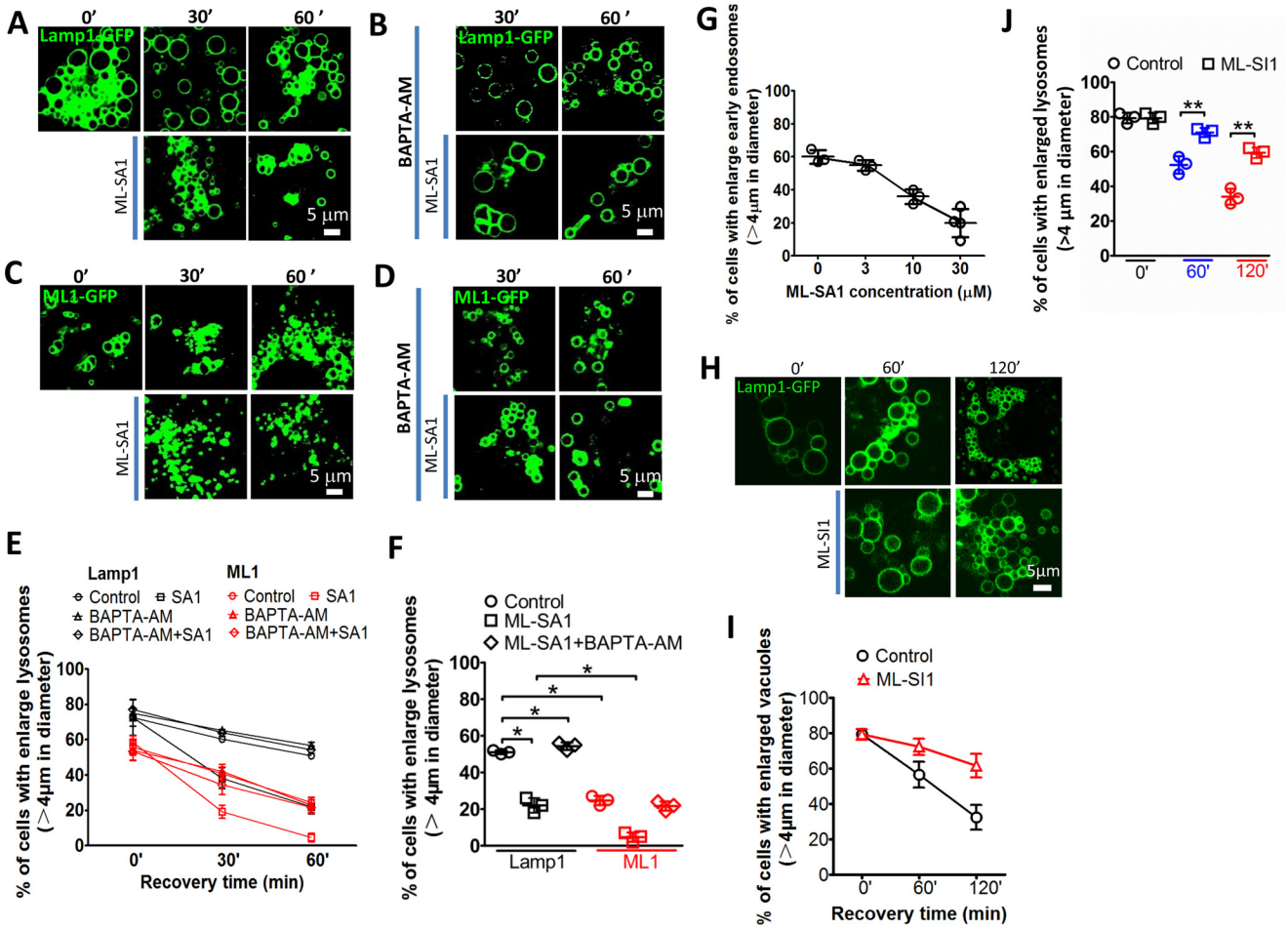

Figure 2. Activation of TRPML1 enhances lysosome recovery from vacuolation induced by vacuolin-1. *A*, Lamp1-GFP-expressing Cos1 cells were treated with vacuolin-1 for 4 h and then rinsed and supplied with fresh medium with or without ML-SA1 (15 μM). Images were taken at 0, 30, and 60 min after vacuolin-1 removal. ML-SA1 promoted enlarged lysosomes to restore normal size. *B*, Ca^{2+} chelation with membrane-permeable BAPTA-AM (50 μM, co-application with ML-SA1) abolished the effect of ML-SA1 on restoration of lysosome size. *C* and *D*, TRPML1-GFP-expressing Cos1 cells were treated as in *A* and *B*. *E*, percentage of cells containing enlarged lysosomes during the time course of recovery after vacuolin-1 removal as in *A–D*. *F*, histogram summary of percentage of cells containing enlarged lysosomes at 60 min of recovery from vacuolin-1 as in *A–D*. *G*, ML-SA1 promoted enlarged lysosome recovery in a dose-dependent manner. Histograms represent the mean percentages of cells with enlarged lysosomes at 30 min after vacuolin-1 removal at different concentrations. *H*, inhibiting TRPML1 with ML-SI1 (25 μM) significantly suppressed enlarged lysosome recovery when compared with controls from vacuolin-1 treatment. *I*, percentage of cells containing enlarged lysosomes in time course of recovery in *G*. *J*, histogram summary of percentage of cells containing enlarged lysosomes at 60 min of recovery from vacuolin-1 as in *H*. The experiment was repeated three times, and representative fluorescence images are shown. *Error bars* represent S.D. *NS*, no significance; *, $p < 0.05$; **, $p < 0.01$.

by MA in P2X4-expressing cells were dramatically suppressed by TRPML1 overexpression. The percentage of P2X4-expressing cells with enlarged lysosomes (induced by MA) was decreased from 79.00 ± 2.64 to 30.00 ± 2.66% by TRPML1 co-expression. In contract, co-expression of two-pore channel 2 (TPC2), a Na^+ release channel (37–39), and TRPML1-DDKK, a non-conducting TRPML1 mutant (21), did not increase the percentage of cells with enlarged lysosomes induced by MA in P2X4-expressing cells (Fig. 3*B*), suggesting that lysosome size is specifically controlled by TRPML1.

Next, we tested whether the enlargement of lysosomes induced by activation of endogenous P2X4 could also be rescued by TRPML1 up-regulation. Lysosomes were labeled with Lamp1-GFP. MA-induced enlarged lysosomes were observed in 35.33 ± 6.81% Cos1 cells expressing Lamp1-GFP (Fig. 3*C*). Overexpression of TRPML1 but not TRPML1-DDKK (Fig. 3*D*) decreased the lysosome size induced by activation of endogenous P2X4. The percentage of cells with enlarged lysosomes was decreased to 6.67 ± 3.06% by TRPML1 expression and to 7.67 ± 5.51% by ML-SA1 treatment, respectively (Fig. 3*C*).

The pH-dependent regulation of P2X4 channel activity can be eliminated by a H286A mutation (12, 40). We have shown that Cos1 cells expressing rP2X4-H286A-GFP exhibit enlarged lysosomes in the absence of MA treatment (12). In agreement with the data from cells expressing P2X4, enlarged lysosomes in cells expressing rP2X4-H286A-GFP was reduced by either ML-SA1 treatment or TRPML1 expression, with a decrease in the percentage of cells with enlarged lysosomes from 69.67 ± 4.04 to 22.67 ± 6.81 and 19.00 ± 3.11%, respectively (Fig. 3*E*). In contrast, co-expression of either TPC2 or TRPML1-DDKK did not decrease the percentage of cells with enlarged lysosomes (data not shown).

Activation of TRPML1 potentiates the recovery of lysosomes induced by P2X4 up-regulation

We also investigated the recovery of enlarged lysosomes induced by MA in cells overexpressing P2X4. As shown in Fig.

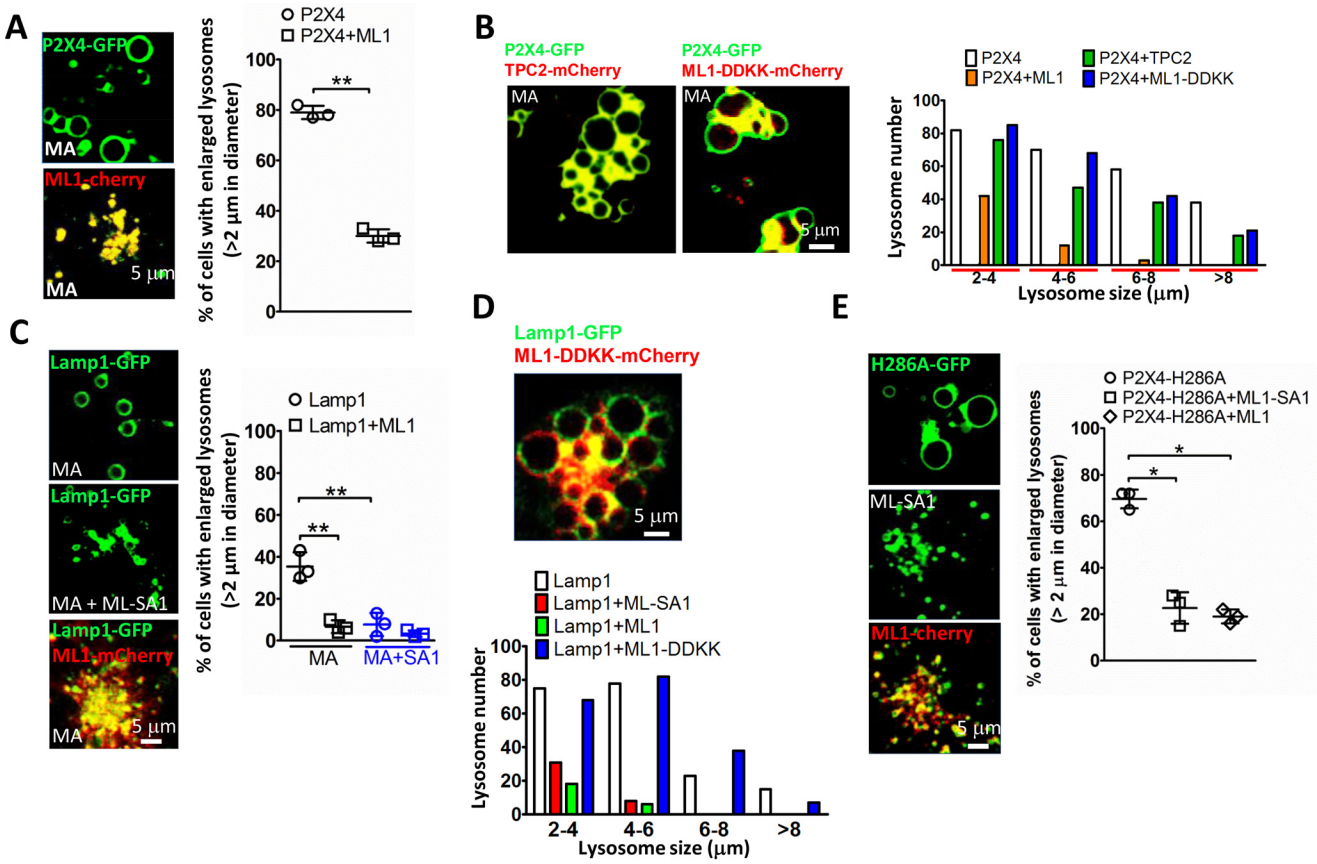

Figure 3. TRPML1 up-regulation abolished lysosome enlargement induced by MA in Cos1 cells expressing P2X4-GFP. *A*, MA (10 mM)-induced lysosome enlargement in P2X4-GFP-expressing Cos1 cells was inhibited by TRPML1-mCherry co-expression. A summary of percentage of cells containing enlarged lysosomes is shown on the *right*. *B*, TPC2 or TRPML1-DDKK does not inhibit MA-induced lysosome enlargement in P2X4-GFP-expressing Cos1 cells. The histogram of lysosome size distributions shows that enlarged lysosomes induced by MA in P2X4-expressing cells were not inhibited by co-expression of TPC2, a Na^+ release channel, or TRPML1-DDKK, a non-conducting TRPML1 mutant. The data were pooled from 21 cells. *C*, activation of endogenous P2X4 by MA resulted in enlarged lysosomes that were labeled with Lamp1-GFP. Either activating TRPML1 with ML-SA1 or TRPML1 overexpression prevented MA from inducing enlarged lysosomes. A summary of percentage of cells containing enlarged lysosomes is shown on the *right*. *D*, TRPML1-DDKK cannot prevent MA-induced lysosome enlargement in Lamp1-GFP-expressing Cos1 cells. The histogram of lysosome size distributions shows that ML-SA1 (15 μM) or TRPML1 overexpression but not TRPML1-DDKK inhibited the enlarged lysosomes induced by MA in Lamp1-GFP-expressing cells. The data were pooled from 20 cells. *E*, ML-SA1 treatment or TRPML1-mCherry expression eliminated enlarged lysosomes in Cos1 cells expressing P2X4-H286A-GFP (pH insensitive gain-of-function mutant of P2X4). A summary of percentage of cells containing enlarged lysosomes is shown on the *right*. The experiment was repeated three times, and representative fluorescence images are shown. The cells were counted as described under "Experimental procedures." *Error bars* represent S.D. *NS*, no significance; *, $p < 0.05$; **, $p < 0.01$.

4 (*A* and *B*), the percentage of P2X4-expressing cells with enlarged lysosomes was reduced from 69.33 ± 3.79 to 41.00 ± 2.65% after 90 min of MA removal. ML-SA1 treatment remarkably increased the recovery speed, and the percentage of cells with enlarged lysosomes was reduced from 69.33 ± 3.79 to 7.67 ± 2.52% after 90 min of MA removal. This was reversed by BAPTA-AM, in which the percentage of cells with enlarged lysosomes returned to 36.33 ± 3.51% (Fig. 4, *A*–*C*). Consistently, ML-SA1 treatment reduced lysosome size in cells expressing H286A-GFP, and this was eliminated by BAPTA-AM (Fig. 4, *D*–*F*). The percentage of H286A-GFP-expressing cells with enlarged lysosomes was reduced from 69.35 ± 4.04 to 20.67 ± 3.79% by ML-SA1 treatment for 120 min, and BAPTA-AM reversed the percentage back to 55.33 ± 8.50%.

TRPML1 deficiency leads to enlarged lysosomes and slower recovery of enlarged lysosomes

By using electron microscopy, deficiency in TRPML1 has been shown to cause enlarged lysosomes (10). In agreement with this, more spontaneously enlarged lysosomes were revealed in TRPML1-deficient (ML4) human fibroblasts than in wild-type fibroblasts under confocal microscope. Enlarged lysosomes (>2 μm) were observed in only 0.33 ± 0.58% of wild-type cells but in 16.33 ± 6.11% of ML4 cells (Fig. 5, *A* and *B*). Vacuolin-1 treatment for 3 h dramatically increased the percentage of cells with enlarged lysosomes, with 41.33 ± 15.31% in wild-type cells but 91.33 ± 3.51% in ML4 cells (Fig. 5, *A* and *C*). Further increasing the treatment time of vacuolin-1 to 6 h caused similar percentages of cells with enlarged lysosomes in both wild-type and ML4 cells (91.00 ± 3.61% in wild-type cells and 94.00 ± 2.10% in ML4 cells, respectively; Fig. 5, *A* and *D*). This allows us to further investigate whether TRPML1 is required for the recovery of enlarged lysosomes in both wild-type and ML4 cells. Both wild-type and ML4 cells were first treated with vacuolin-1 for 6 h to induce similar sizes of enlarged lysosomes, and then the percentage of cells with enlarged lysosomes was compared at 6 h after vacuolin-1 removal. Notably, the percentage of cells with enlarged lysosomes after 6 h of recovery was reduced to 6.00 ± 4.58% in

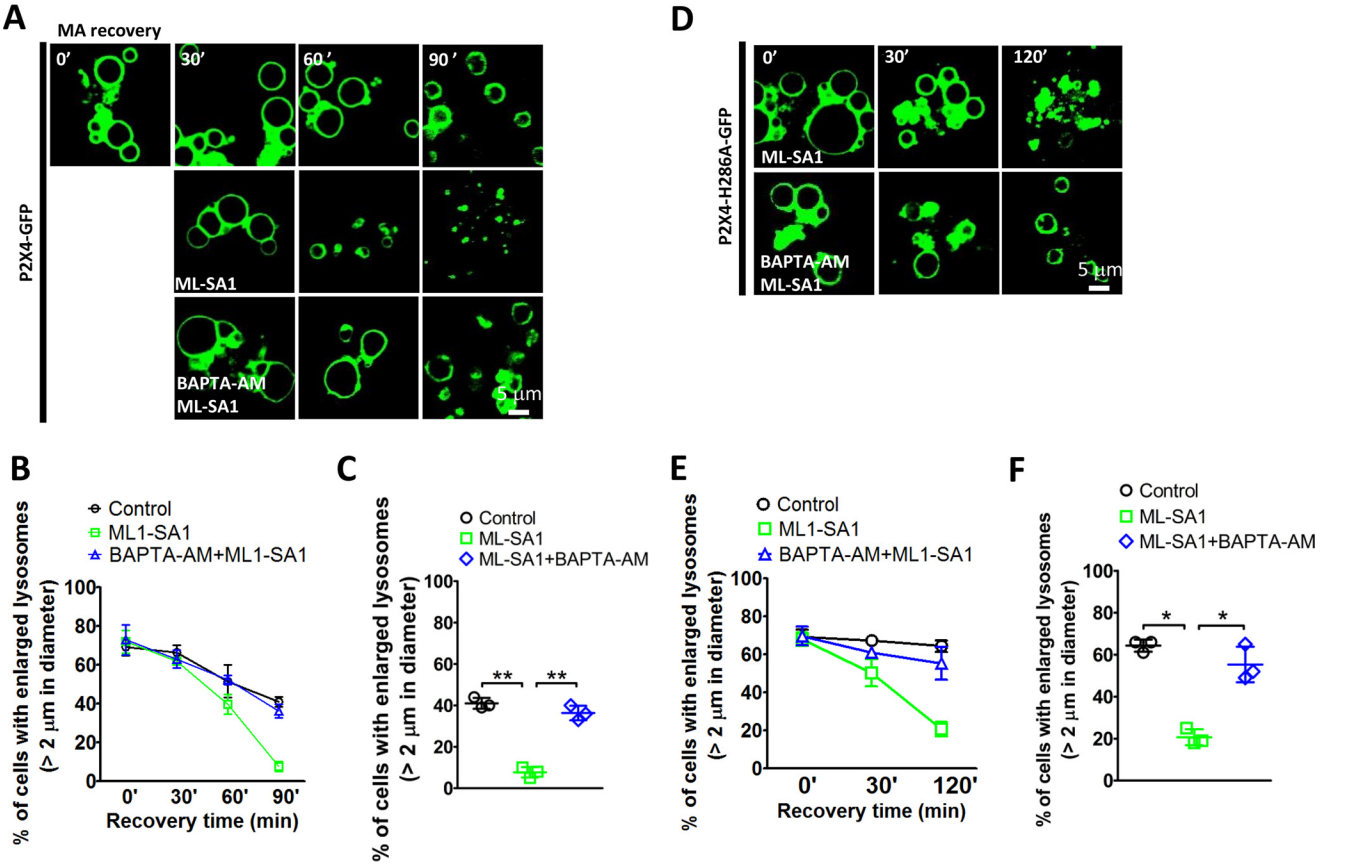

Figure 4. TRPML1 activation enhances lysosome recovery from vacuolation induced by MA in Cos1 cells expressing P2X4-GFP. *A*, P2X4-GFP-expressing Cos1 cells were treated with MA for 2 h and then rinsed and supplied with fresh medium with or without ML-SA1 (15 μM). Images were taken at 0, 60, and 90 min of recovery. ML-SA1 promoted enlarged lysosome recovery, and this was abolished by co-applying BAPTA-AM. *B*, percentage of cells containing enlarged lysosomes (>2 μm in diameter) in time course of recovery as in *A*. *C*, percentage of cells containing enlarged lysosomes at 90 min of recovery from MA. *D*, ML-SA1 treatment reduced enlarged lysosomes in Cos1 cells expressing P2X4-H286A-GFP, and this was inhibited by BAPTA-AM. *E*, percentage of cells containing enlarged lysosomes in time course of ML-SA1 treatment. *F*, percentage of cells containing enlarged at 120 min of ML-SA1 treatment. The experiment was repeated three times, and representative fluorescence images are shown. The cells were counted as described under "Experimental procedures." *Error bars* represent S.D. *NS*, no significance; *, $p < 0.05$; **, $p < 0.01$.

wild-type cells but to only 79.33 ± 7.02% in ML4 cells (Fig. 5*E*). Additionally, the enlarged lysosomes in ML4 cells were rescued by TRPML1 overexpression (Fig. 5, *A*–*E*). Taken together, our data suggest that TRPML1 may be required for lysosome fission.

TRPML1 modulates lysosome size via regulating CaM

Both TRPML1 and P2X4 are Ca^{2+}-permeable channels located in the lysosomal membrane. How lysosomes differentiate the two Ca^{2+} release processes and respond with opposite consequences remains a fascinating question. One possibility is that the fission and fusion machineries utilize different Ca^{2+} sensors. Currently, three Ca^{2+}-binding proteins, CaM (6, 41), synaptotagmin VII (Syt VII) (42), and ALG-2 (43) have been proposed to function as Ca^{2+} sensors that regulate intracellular membrane trafficking. We have shown that CaM but not Syt VII and ALG-2 senses the Ca^{2+} released via P2X4 to initiate lysosomal fusion (12). It remains to be determined which Ca^{2+} sensor is involved in TRPML1-mediated fission. Given that ALG-2 (43, 44) but not Syt VII (Fig. 6A) binds to TRPML1 and regulates its effect on lysosome trafficking, we tested whether ALG-2 regulates lysosome size. We found that deleting ALG-2 using CRISPR/Cas9 strategy (12) (Fig. 6, *B* and *C*) had no effect on enlarged lysosome recovery. To further test whether ALG-2 was involved in TRPML1-mediated fission, we applied ML-SA1 during the recovery phase. ALG-2 deletion (Fig. 6, *D* and *E*) did not significantly suppress the facilitating effect of ML-SA1 on lysosome recovery. Altogether, these data suggest that ALG-2 may not contribute to TRPML1-mediated fission.

Interestingly, inhibiting CaM with W7 (3 mM) prevented vacuolin-1 induced enlarged lysosomes from recovery. The facilitation of enlarged lysosome recovery by activating TRPML1 with ML-SA1 was also inhibited by suppressing W7 (Fig. 7, *A* and *B*). These data suggest that CaM may be required for TRPML1-mediated lysosome fission. Supporting this, a stronger association between TRPML1 and CaM during enlarged lysosome recovery was revealed, as compared with normal or vacuolin-1 treatment condition. This was suppressed by either ML-SI1 or BAPTA-AM (Fig. 7*C*). These data suggest that during enlarged lysosome recovery TRPML1 may be activated to release Ca^{2+}, thereby increasing its association with CaM. Consistently, activating TRPML1 using ML-SA1 also increased the association between TRPML1 and CaM, and this was inhibited by BAPTA-AM (Fig. 7*C*). As a control, the association between P2X4 and CaM was not increased during enlarged lysosome recovery (Fig. 7*D*). Taken together, our data

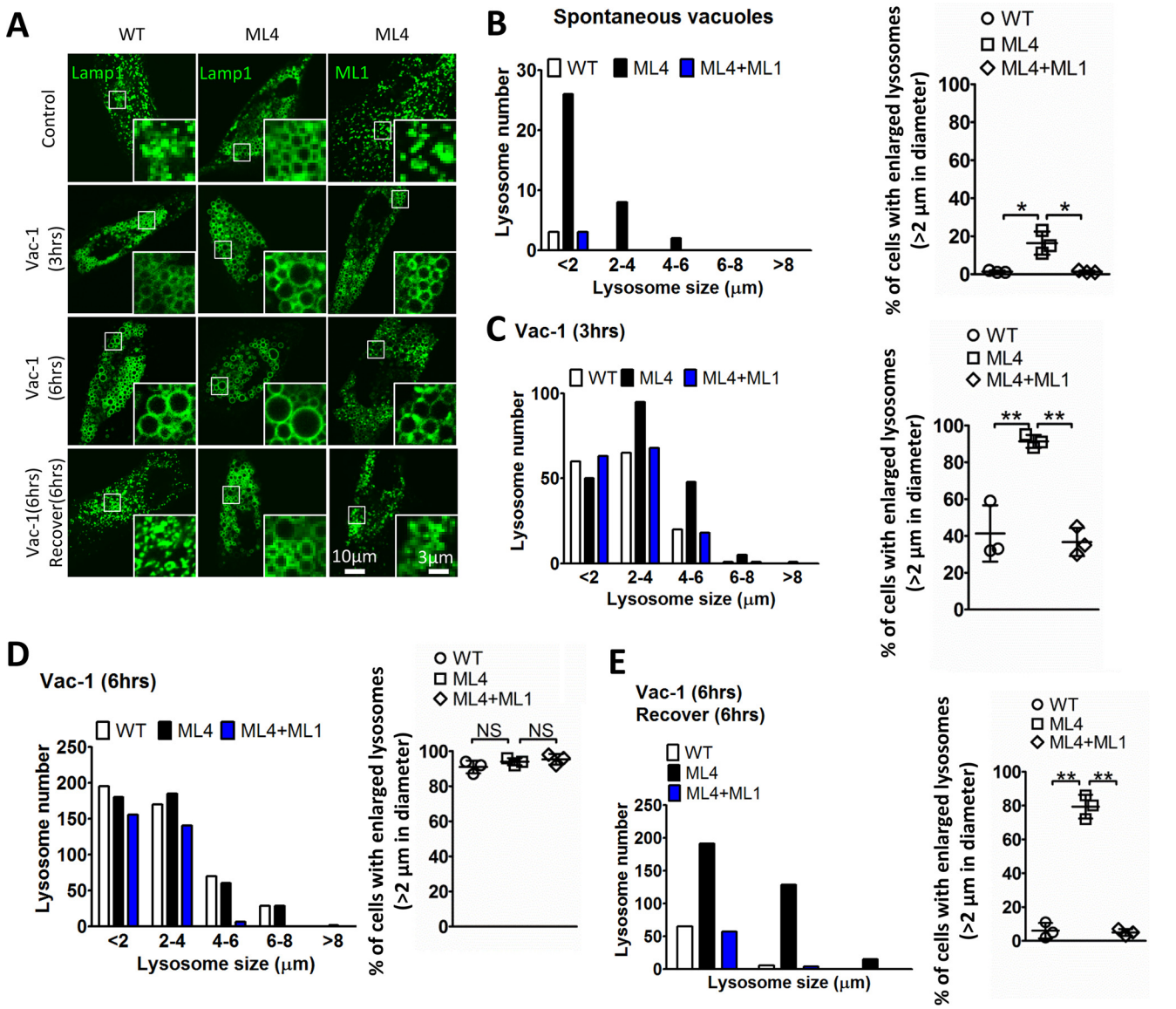

Figure 5. TRPML1-deficient human skin fibroblasts show enlarged lysosomes. *A*, TRPML1$^{-/-}$ (ML4) fibroblasts (GM02629) showed significantly enlarged lysosomes, either at rest (*first row*), upon vacuolin-1 (3 h) (*second row*), upon vacuolin-1 (6 h) (*third row*), or at 6 h during recovery from vacuolin-1 (*fourth row*), compared with wild-type human skin fibroblasts (GM00969). The experiment was repeated three times, and representative differential interference contrast images from confocal are shown. TRPML1 overexpression rescued the enlarged lysosomes in ML4 cells. *B*, statistics analysis of spontaneous enlarged lysosomes in wild-type and ML4 fibroblasts. *Left panel*, histogram of lysosome size distributions pooled from 16 fibroblasts; *right panel*, summary of percentage of cells containing enlarged lysosomes >2 μm in diameter (in parallel with *first row* in *A*). *C*, statistics analysis of enlarged lysosomes induced by 3 h of vacuolin-1 (1 μM) treatment (in parallel with the *second row* in *A*). *D*, statistics analysis of enlarged lysosomes induced by 6 h of vacuolin-1 treatment. 6 h of vacuolin-1 induced a comparable lysosome enlargement between wild-type and ML4 fibroblasts (in parallel with the *third row* in *A*). *E*, percentage of cells containing enlarged lysosomes at 6 h during recovery from vacuolin-1 for 6 h (in parallel with *fourth row* in *A*). After 6 h of vacuolin-1 treatment, fibroblasts were rinsed with fresh warm medium three times and then incubated in fresh medium to allow cells recovering for another 6 h. The experiment was repeated three times independently, and cells were counted as described under "Experimental procedures." *Error bars* represent S.D. *NS*, no significance; *, $p < 0.05$; **, $p < 0.01$.

suggest that TRPML1 activation may increase lysosome fission by activating CaM.

Discussion

Intracellular lysosomal membrane trafficking, including fusion and fission, is an important cellular process. Compared with the fusion process, very limited information is available for lysosomal membrane fission. Recent studies have shown that Ca^{2+} release via lysosomal P2X4 activates CaM to trigger lysosome fusion (12). However, the molecular identities of the Ca^{2+} release channel and the Ca^{2+} sensor(s) controlling lysosome fission remain unclear. By using different methods, including lysosome-patch-clamping (14, 15), Fura-2-based Ca^{2+} imaging (17–19), genetic-encoded Ca^{2+} sensors (GCamp-TRPML1 (17, 20) or GECO-TRPML1 (21)), and lipid bilayers (25–28), TRPML1 has been demonstrated to be a Ca^{2+}-permeable channel in the lysosome. In this study, we investigated the role of TRPML1 in the regulation of lysosome size. We found that an increase in TRPML1 activity promoted enlarged lysosome recovery, suggesting a role of TRPML1 in lysosome fission. In agreement with the results above, TRPML1-deficient cells displayed enlarged lysosomes, and the recovery of enlarged

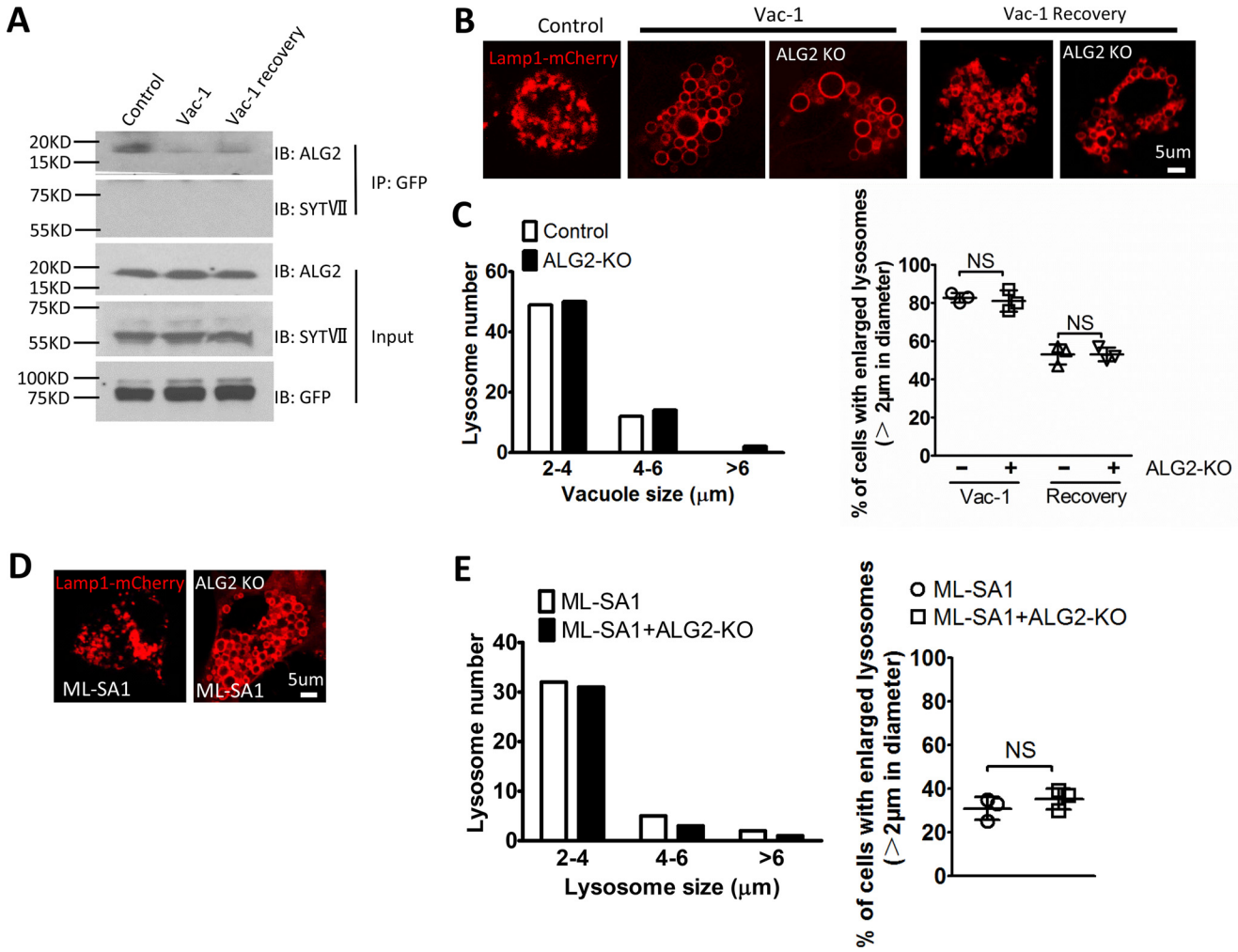

Figure 6. ALG-2 and Syt VII are not involved in the effect of TRPML1 in lysosome size control. *A*, ALG-2 but not Syt VII interacts with TRPML1. HEK293T cells were transfected with TRPML1-GFP. The cells were lysed by adding 0.5% Triton X-100. The samples were immunoprecipitated with protein A/G-anti-GFP and blotted with anti-ALG-2 and anti-Syt VII. A weaker association between TRPML1 and ALG-2 was detected under vacuolin-1 (1 μM, 2 h) treatment or during lysosome recovery from vacuolin-1 treatment. No interaction between TRPML1 and Syt VII was detected under all three conditions. *B–E*, ALG-2 is not involved in TRPML1-mediated lysosome fission. *B* and *C*, HEK-293T cells were transiently transfected with Lamp1-mCherry, co-transfected with or without ALG-2-KO. Ablating ALG-2 using CRISPR/Cas9 strategy in HEK293T cells had no effect on enlarged lysosome recovery. The data for vacuole size distribution was pooled from 20 cells for each condition. A summary of the percentage of cells containing enlarged lysosomes (at least three lysosomes of >2 μm in diameter) from three independent experiments is shown, and >250 cells were counted for each experiment. *D* and *E*, the effect of ML-SA1 on enlarged lysosome recovery was not affected by ALG-2 deletion in HEK293T cells. The data for vacuole size distribution was pooled from 20 cells for each condition. A summary of the percentage of cells containing enlarged lysosomes (at least three lysosomes of >2 μm in diameter) from three independent experiments is shown, and >250 cells were counted for each experiment. *IB*, immunoblot.

lysosomes was slower in TRPML1 mutant cells after vacuolin-1 removal. Furthermore, we showed that TRPML1 strongly associated with CaM during enlarged lysosome recovery, and the regulation of lysosome size by TRPML1 was dependent on both Ca^{2+} and CaM. Our data suggest that TRPML1 activation may promote lysosome fission by activating CaM. Given that lysosome fission is implicated in lysosome biogenesis and reformation (7, 45), this finding suggests that TRPML1 may function as the key lysosomal Ca^{2+} channel regulating autophagic lysosome reformation[4] (44, 45) or lysosome biogenesis (7, 30, 32). In general, our results are in agreement with previous reports, including that 1) TRPML1-null mutant cells display enlarged lysosomes and defects in lysosome biogenesis (10, 29, 30, 32); and 2) an increase in PI(3,5)P2, an endogenous agonist of TRPML1, promotes vacuole fission (33), whereas the deficiency in PI(3,5)P2 causes vacuole enlargement in both yeast (33, 34) and mammalian cells (14).

Because TRPML1 is a nonselective cation channel that permeates Ca^{2+}, Na^{+}, and other cations (15), we cannot exclude the possible contribution of Na^{+} and other cations in regulating lysosome fission. In particular, earlier studies suggest that TRPML1 functions as a lysosomal H^{+} channel (46, 47). However, the contribution of other cations might be minimal because: 1) TRPML1 regulating lysosome fission was compromised by Ca^{2+} chelator BAPTA-AM (Fig. 2, *E* and *F*), 2) the lysosomal Na^{+} channel TPC2 (37–39) had no effect on lysosomal fission (Fig. 3*B*), 3) the recovery of enlarged lysosomes was strongly suppressed by inhibiting the prototypical Ca^{2+} sensor CaM (Fig. 7), 4) lysosomal lumen accumulates mainly Na^{+} and Ca^{2+} (37, 48), 5) lysosomal membrane biogenesis and

[4] Q. Cao, Y. Yang, X. Z. Zhong, and X.-P. Dong, unpublished data.

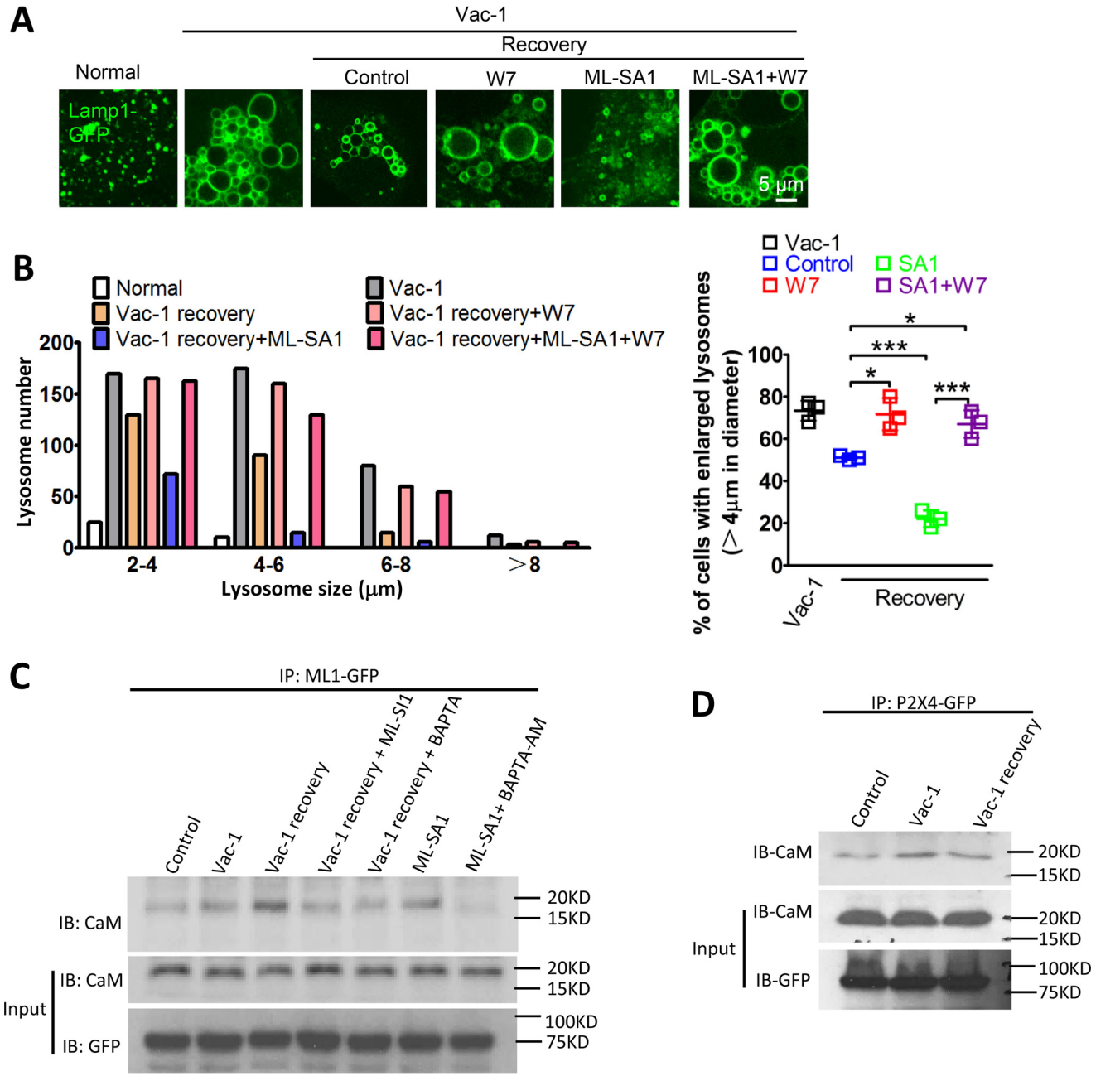

Figure 7. CaM in involved in the effect of TRPML1 in lysosome size control. *A*, lysosomes were enlarged by vacuolin-1, and then vacuolin-1 was removed to allow cells to recover for 1 h. ML-SA1 facilitated the recovery of enlarged lysosomes, which was inhibited by CaM inhibitor W7 (3 μM). *B*, histogram for lysosome size distributions pooled from 20 cells, and summary of percentage of cells containing enlarged lysosomes >4 μm in diameter. The experiment was repeated three times, and the cells were counted as described under "Experimental procedures." *Error bars* represent S.D. *NS*, no significance; *, $p < 0.05$; **, $p < 0.01$. *C*, in HEK293T cells, a stronger association between TRPML1 and CaM during lysosome recovery from vacuolin-1 treatment (1 μM, 2 h) as compared with cells under vacuolin-1 treatment. This was abolished by either ML-SI1 or BAPTA-AM. Activation of TRPML1 by ML-SA1 also increased the association between TRPML1 and CaM, and this was inhibited by BAPTA-AM. *D*, the association between P2X4 and CaM was not significantly changed during the recovery of enlarged lysosome in HEK293T cells transfected with P2X4-GFP. *IB*, immunoblot; *IP*, immunoprecipitation.

reformation are dependent on lysosomal Ca^{2+} (5, 7, 20, 30–32), and 6) later studies demonstrate that TRPML1 is not a H^+-permeable channel (15, 49–51).

In this study, Lamp1 GFP is used as a marker to detect lysosome size. Lamp1-GFP overexpression could be misdirected to other cellular organelles such as endosomes, or TRPML1 may regulate lysosome size by affecting endosome-lysosome fusion. However, because TRPML1 deficiency only causes defect in the late endocytic pathways (10, 29), because reducing TRPML1 levels results in a delay and not a block in the transport events (52), and because vacuolin-1 induced vacuoles are derived from early endosomes and lysosomes by homotypic fusion (53), it is unlikely that TRPML1 regulates lysosome size by affecting endosome-lysosome fusion. In accord, neither down-regulating ($TRPML1^{-/-}$ and ML-SI1) nor up-regulating (ML-SA1) TRPML1 had an effect on early endosome size, although lysosome size was altered by regulating TRPML1 (supplemental Fig. S1). Consistent with previous studies (53), vacuolin-1

enlarged both early endosomes and lysosomes. In the presence of vacuolin-1, TRPML1 regulated lysosome size but not early endosome size (supplemental Fig. S1). Therefore, TRPML1 specifically regulates lysosome size.

Both TRPML1 and P2X4 are Ca^{2+}-permeable channels in lysosomes. How the lysosome differentiates the two Ca^{2+}-release processes with opposite responses remains an interesting question. Particularly, it is intriguing how two different Ca^{2+} channels use the same Ca^{2+} sensor, CaM, to regulate two opposite events. One possibility is that the conditions favoring their activation are distinct. TRPML1 is activated by acidic pH (15), whereas P2X4 is activated by alkaline pH in the lumen (12, 54). We speculate that possibly segregated subdomains responsible for fusion and fission exist on the lysosomal membrane. The "fusion subdomain" may be enriched of P2X4, whereas the "fission subdomain" may contain abundant TRPML1. During lysosome fission, V-ATPase may be recruited to the fission subdomain, which may cause a decrease of the local pH and in turn enhance Ca^{2+} release through TRPML1 to activate CaM (55) and trigger fission. For fusion, the V-ATPase may be removed from the fusion subdomain, leading to an increase of the local pH and a consequent activation of P2X4, which signals through CaM to initiate fusion. Supporting the subdomain model, previous studies have suggested that fusion requires the physical presence of the membrane sector (V0) of the vacuolar H^+-ATPase, but not its pump activity. Lysosome fission, in contrast, depends on H^+ translocation by the V-ATPase (56, 57). This is also supported by our unpublished observations[4] that no single channel activity has been detected in lysosome-attached, luminal-side-out, and cytosol-side-out patches, although such an activity has been measured on the plasma membrane (58, 59). This indicates that these channels are clustered on the lysosomal membrane. Unfortunately, because of the spatial resolution limit of light microscopy (~0.2 μm), it is impossible for us to experimentally demonstrate this using confocal microscopy. The delicate balance between P2X4/fusion and TRPML1/fission should be an interesting topic for further investigation.

It is unclear why CaM associates with TRPML1 during enlarged lysosome recovery but associates with P2X4 during vacuolin-1 treatment that induces lysosome fusion. Given that vacuolin-1 alkalinizes lysosomal pH (60) and P2X4 is activated by an increase in lysosomal pH (61), we would reason that vacuolin-1 promotes P2X4 activity via alkalinizing lysosomes, thereby increasing its association with CaM (Fig. 7*D*) (12). Conversely, during vacuolin-1 removal, V-ATPase activity may be increased to reacidify lysosomes. This leads to elevated TRPML1 activity and its association with CaM (Fig. 7*C*).

Finally, TPC2 has also been implicated in lysosomal Ca^{2+} release in response to nicotinic acid adenine dinucleotide phosphate (8, 9, 37–39, 62–71). However, we did not observe an effect of TPC2 in regulating lysosome fission. Previous studies even showed that TPC2 overexpression enlarged lysosomes in Cos1 cells (37). Potentially, TPC2-mediated Na^+ release may rapidly depolarize endolysosomal membranes to facilitate membrane fusion (37).

Experimental procedures

Cell culture

Cos1 and HEK293T cells were obtained from ATCC (Manassas, VA) and maintained in Dulbecco's modified Eagle's medium/nutrient mixture F-12 (DMEM/F12) supplemented with 10% FBS (Invitrogen). The cells were cultured at 37 °C in a 5% CO_2 atmosphere. Wild-type human skin fibroblasts (GM00969) and ML4 fibroblasts (GM02629) were obtained from Coriell Institute and maintained in DMEM supplemented with 10% FBS. For some experiments, cells were seeded on 0.1% polylysine-coated coverslips and cultured for 24 h before further experiments. Cells from passage numbers 5–25 were used for subsequent assays.

Antibodies and reagents

The antibodies used for Western blotting were rabbit anti-CaM (1:2000; Abcam) and mouse anti-GFP (1:1000; Thermo Scientific). HRP-conjugated goat anti-rabbit and goat anti-mouse antibodies were purchased from Thermo Fisher Scientific and Bio-Rad Laboratories, Inc., and used at 1:5,000 and 1:10,000 dilutions, respectively.

The following chemicals were used in the present study: Texas Red 10-kDa dextran (Invitrogen; 1 mg/ml) used to label late endosomes and lysosomes; MA (10 mM, pH adjusted to 7.4 with HCl; Sigma); bafilomycin A1 (200 nM; Tocris Bioscience, Bristol, UK); vacuolin-1 (1 μM; Santa Cruz Biotechnology, Inc.); W7 (3 μM; Sigma); BAPTA-AM (10 μM; Invitrogen); ML-SA1 (15 μM; Tocris Bioscience); and ML-SI1 (15 μM. Enzo Life Sciences Inc.).

Confocal microscopy

Confocal fluorescent images were taken using an inverted Zeiss LSM510 Axiovert 200Ms confocal microscope with a 40× or 63× oil-immersion objective at room temperature. Sequential excitation wavelengths at 488 and 543 nm were provided by argon and helium-neon gas lasers, respectively. Emission filters BP515-565 and LP590 were used for collecting green and red images in channels 1 and 2, respectively. After sequential excitation, green and red fluorescent images of the same cell were saved with ZEN2012 software. The images were analyzed by Zeiss software. The term co-localization refers to the coincident detection of above-background green and red fluorescent signals in the same region.

Molecular biology and biochemistry

Rat P2X4 receptor with enhanced GFP fused to the C terminus (rP2X4-GFP). Briefly, for rP2X4-GFP, the rat P2X4 cDNA was amplified by polymerase chain reaction using oligonucleotide primers to introduce a Kozak initiation sequence (73), remove the stop codon, and introduce NheI and SacII sites at the 5′ and 3′ ends, respectively. Amplification products were then cloned into the pEGFP-N1 vector (Addgene, Cambridge, MA). The transgene length is 1164 bp. The H286A point mutations were made using a site-directed mutagenesis kit (Qiagen). The sequences of all amplified regions were verified using automated DNA sequencing (GENEWIZ, South Plainfield, NJ). Full-length mouse TRPML1 was cloned into the EGFP-C2

(Clontech) or mCherry vector (14). TRPML1 non-conducting pore mutant (D471K/D472K; abbreviated TRPML1-DDKK) was constructed using a site-directed mutagenesis kit (Qiagen). Cloning sites are Nod1 at both 5′ and 3′ ends. The dominant-negative form was generated by introducing D172N and D303N point mutations. Cos1 cells were transiently transfected using Lipofectamine 2000 or 3000 (Invitrogen), which usually reach >85% transfection efficiency.

Immunoprecipitation and Western blotting

Cell lysates (2–5 mg/ml) were incubated with 80 μl of 50% protein A/G-agarose beads in PBS for 15 min at 4 °C to reduce background proteins that non-specifically bound to the beads. After centrifugation at 12,000 × *g* for 15 min to remove the beads, aliquots of cell lysates (1–2 mg of protein) were incubated with the desired antibodies (3–4 μg) or control IgG at 4 °C overnight in a final volume of 1 ml of radioimmune precipitation assay radioimmune precipitation assay-PBS buffer with constant rocking. After antibody incubation, protein A/G-agarose beads were added, and the samples were incubated at 4 °C for 4 h, followed by centrifugation at 1,500 rpm for 10 min at 4 °C. The beads were then washed three times with precooled radioimmune precipitation assay without proteinase inhibitors and each time were centrifuged at 1,500 rpm for 10 min at 4 °C. Immune complexes were resolved by SDS-PAGE and subjected to immunoblotting. Proteins were analyzed by standard blot Western analysis methods.

Vacuole assay

Cos1 cells were transiently transfected with desired cDNAs. Non-transfected cells or cells transfected with Lamp1 were used as controls. At 24 h after transfection, the cells on coverslips were treated with various chemicals as indicated. After the treatment, they were rinsed and fixed with 4% paraformaldehyde and were mounted to glass slides with coverslips and viewed immediately. All images were taken using a Zeiss Meta510 confocal microscope. Normally, the majority of late endosomes and lysosomes have sizes with diameters less than 0.5 μm, which are hard to resolve with light microscopy. For quantification, the cells were counted as vacuolated if there were more than three enlarged (>2 μm or >4 μm in diameter) cytoplasmic vacuoles, with the vacuole sizes determined using the ZEN 2012 program. The percentage of vacuolated cells in each experiment was calculated from counting at least 250 cells from randomly chosen fields, and the experiments were repeated three times ($n = 3$).

Knock-out of ALG-2 using CRISPR-Cas9 system

The operation followed detailed instructions of the published protocol (72). In brief, 20-bp target single-guide RNA sequences were obtained by screening ALG-2 mRNA with CRISPR DESIGN online software, and two sequences were chosen: GCTGCCTACTCCTACCGCCC (target 1) and TGTCTTCCGGACCTACGACA (target 2). After being annealed with their reverse complementary sequences, the short double-strand DNAs (hereafter named gDNA) were ligated with BbsI-digested pX330–2A-GFP, and the new constructs were named pX330–2A-GFP/ALG-2 gDNA1 and 2, respectively (12).

Data analysis

The data are presented as means ± S.D. Statistical comparisons were made using analysis of variance and Student's *t* test. *p* values of < 0.05 were considered statistically significant. *, $p < 0.05$; **, $p < 0.01$.

Author contributions—Q. C. and Y. Y. performed confocal microscopy and Western blotting experiments and data analysis. X. Z. Z. provided constructive comments on the manuscript. X.-P. D. designed the projects and wrote the manuscript with input from co-authors.

Acknowledgments—We thank Haoxing Xu for constant assistance and support. We are also grateful to Lin Mei for CaM-Myc-His plasmid and Michael X. Zhu for TPC2-mCherry and Lamp1-mCherry. We appreciate the encouragement and helpful comments from other members of the Dong laboratory.

References

1. Saftig, P., and Klumperman, J. (2009) Lysosome biogenesis and lysosomal membrane proteins: trafficking meets function. *Nat. Rev. Mol. Cell Biol.* **10,** 623–635
2. Luzio, J. P., Pryor, P. R., and Bright, N. A. (2007) Lysosomes: fusion and function. *Nat. Rev. Mol. Cell Biol.* **8,** 622–632
3. Luzio, J. P., Bright, N. A., and Pryor, P. R. (2007) The role of calcium and other ions in sorting and delivery in the late endocytic pathway. *Biochem. Soc. Trans.* **35,** 1088–1091
4. Hay, J. C. (2007) Calcium: a fundamental regulator of intracellular membrane fusion? *EMBO Reports* **8,** 236–240
5. Piper, R. C., and Luzio, J. P. (2004) CUPpling calcium to lysosomal biogenesis. *Trends Cell Biol.* **14,** 471–473
6. Peters, C., and Mayer, A. (1998) Ca^{2+}/calmodulin signals the completion of docking and triggers a late step of vacuole fusion. *Nature* **396,** 575–580
7. Pryor, P. R., Mullock, B. M., Bright, N. A., Gray, S. R., and Luzio, J. P. (2000) The role of intraorganellar Ca^{2+} in late endosome-lysosome heterotypic fusion and in the reformation of lysosomes from hybrid organelles. *J. Cell Biol.* **149,** 1053–1062
8. Morgan, A. J., Platt, F. M., Lloyd-Evans, E., and Galione, A. (2011) Molecular mechanisms of endolysosomal Ca^{2+} signalling in health and disease. *Biochem. J.* **439,** 349–374
9. Lloyd-Evans, E., and Platt, F. M. (2011) Lysosomal Ca^{2+} homeostasis: role in pathogenesis of lysosomal storage diseases. *Cell Calcium* **50,** 200–205
10. Cheng, X., Shen, D., Samie, M., and Xu, H. (2010) Mucolipins: intracellular TRPML1–3 channels. *FEBS Lett.* **584,** 2013–2021
11. Pittman, J. K. (2011) Vacuolar Ca^{2+} uptake. *Cell Calcium* **50,** 139–146
12. Cao, Q., Zhong, X. Z., Zou, Y., Murrell-Lagnado, R., Zhu, M. X., and Dong, X. P. (2015) Calcium release through P2X4 activates calmodulin to promote endolysosomal membrane fusion. *J. Cell Biol.* **209,** 879–894
13. Shen, D., Wang, X., and Xu, H. (2011) Pairing phosphoinositides with calcium ions in endolysosomal dynamics: phosphoinositides control the direction and specificity of membrane trafficking by regulating the activity of calcium channels in the endolysosomes. *BioEssays* **33,** 448–457
14. Dong, X. P., Shen, D., Wang, X., Dawson, T., Li, X., Zhang, Q., Cheng, X., Zhang, Y., Weisman, L. S., Delling, M., and Xu, H. (2010) $PI(3,5)P_2$ controls membrane trafficking by direct activation of mucolipin Ca^{2+} release channels in the endolysosome. *Nat. Commun.* **1,** 38
15. Dong, X. P., Cheng, X., Mills, E., Delling, M., Wang, F., Kurz, T., and Xu, H. (2008) The type IV mucolipidosis-associated protein TRPML1 is an endolysosomal iron release channel. *Nature* **455,** 992–996
16. Venkatachalam, K., Wong, C. O., and Zhu, M. X. (2015) The role of TRPMLs in endolysosomal trafficking and function. *Cell Calcium* **58,** 48–56
17. Shen, D., Wang, X., Li, X., Zhang, X., Yao, Z., Dibble, S., Dong, X. P., Yu, T., Lieberman, A. P., Showalter, H. D., and Xu, H. (2012) Lipid storage disorders block lysosomal trafficking by inhibiting a TRP channel and lysosomal calcium release. *Nat. Commun.* **3,** 731

18. Lee, J. H., McBrayer, M. K., Wolfe, D. M., Haslett, L. J., Kumar, A., Sato, Y., Lie, P. P., Mohan, P., Coffey, E. E., Kompella, U., Mitchell, C. H., Lloyd-Evans, E., and Nixon, R. A. (2015) Presenilin 1 maintains lysosomal Ca^{2+} homeostasis via TRPML1 by regulating vATPase-mediated lysosome acidification. *Cell Reports* **12,** 1430–1444
19. Kilpatrick, B. S., Yates, E., Grimm, C., Schapira, A. H., and Patel, S. (2016) Endo-lysosomal TRP mucolipin-1 channels trigger global ER Ca^{2+} release and Ca^{2+} influx. *J. Cell Sci.* **129,** 3859–3867
20. Medina, D. L., Di Paola, S., Peluso, I., Armani, A., De Stefani, D., Venditti, R., Montefusco, S., Scotto-Rosato, A., Prezioso, C., Forrester, A., Settembre, C., Wang, W., Gao, Q., Xu, H., Sandri, M., *et al.* (2015) Lysosomal calcium signalling regulates autophagy through calcineurin and TFEB. *Nat. Cell Biol.* **17,** 288–299
21. Cao, Q., Zhong, X. Z., Zou, Y., Zhang, Z., Toro, L., and Dong, X. P. (2015) BK channels alleviate lysosomal storage diseases by providing positive feedback regulation of lysosomal Ca^{2+} release. *Dev. Cell* **33,** 427–441
22. Dayam, R. M., Saric, A., Shilliday, R. E., and Botelho, R. J. (2015) The phosphoinositide-gated lysosomal Ca^{2+} channel, TRPML1, is required for phagosome maturation. *Traffic* **16,** 1010–1026
23. Cheng, X., Zhang, X., Gao, Q., Ali Samie, M., Azar, M., Tsang, W. L., Dong, L., Sahoo, N., Li, X., Zhuo, Y., Garrity, A. G., Wang, X., Ferrer, M., Dowling, J., Xu, L., *et al.* (2014) The intracellular Ca^{2+} channel MCOLN1 is required for sarcolemma repair to prevent muscular dystrophy. *Nat. Med.* **20,** 1187–1192
24. Puertollano, R., and Kiselyov, K. (2009) TRPMLs: in sickness and in health. *Am. J. Physiol. Renal Physiol.* **296,** F1245–F1254
25. Zhang, F., and Li, P. L. (2007) Reconstitution and characterization of a nicotinic acid adenine dinucleotide phosphate (NAADP)-sensitive Ca^{2+} release channel from liver lysosomes of rats. *J. Biol. Chem.* **282,** 25259–25269
26. Guse, A. H. (2012) Linking NAADP to ion channel activity: a unifying hypothesis. *Sci. Signal.* **5,** pe18
27. Zhang, F., Xu, M., Han, W. Q., and Li, P. L. (2011) Reconstitution of lysosomal NAADP-TRP-ML1 signaling pathway and its function in TRP-ML1(−/−) cells. *Am. J. Physiol. Cell Physiol.* **301,** C421–C430
28. Xu, M., Li, X., Walsh, S. W., Zhang, Y., Abais, J. M., Boini, K. M., and Li, P. L. (2013) Intracellular two-phase Ca^{2+} release and apoptosis controlled by TRP-ML1 channel activity in coronary arterial myocytes. *Am. J. Physiol. Cell Physiol.* **304,** C458–C466
29. Chen, C. S., Bach, G., and Pagano, R. E. (1998) Abnormal transport along the lysosomal pathway in mucolipidosis, type IV disease. *Proc. Natl. Acad. Sci. U.S.A.* **95,** 6373–6378
30. Miller, A., Schafer, J., Upchurch, C., Spooner, E., Huynh, J., Hernandez, S., McLaughlin, B., Oden, L., and Fares, H. (2015) Mucolipidosis type IV protein TRPML1-dependent lysosome formation. *Traffic* **16,** 284–297
31. Campbell, E. M., and Fares, H. (2010) Roles of CUP-5, the *Caenorhabditis elegans* orthologue of human TRPML1, in lysosome and gut granule biogenesis. *BMC Cell Biol.* **11,** 40
32. Treusch, S., Knuth, S., Slaugenhaupt, S. A., Goldin, E., Grant, B. D., and Fares, H. (2004) Caenorhabditis elegans functional orthologue of human protein h-mucolipin-1 is required for lysosome biogenesis. *Proc. Natl. Acad. Sci. U.S.A.* **101,** 4483–4488
33. Efe, J. A., Botelho, R. J., and Emr, S. D. (2005) The Fab1 phosphatidylinositol kinase pathway in the regulation of vacuole morphology. *Curr. Opin. Cell Biol.* **17,** 402–408
34. Rudge, S. A., Anderson, D. M., and Emr, S. D. (2004) Vacuole size control: regulation of PtdIns(3,5)P2 levels by the vacuole-associated Vac14-Fig 4 complex, a PtdIns(3,5)P2-specific phosphatase. *Mol. Biol. Cell* **15,** 24–36
35. Huynh, C., and Andrews, N. W. (2005) The small chemical vacuolin-1 alters the morphology of lysosomes without inhibiting Ca^{2+}-regulated exocytosis. *EMBO Reports* **6,** 843–847
36. Grimm, C., Jörs, S., Saldanha, S. A., Obukhov, A. G., Pan, B., Oshima, K., Cuajungco, M. P., Chase, P., Hodder, P., and Heller, S. (2010) Small molecule activators of TRPML3. *Chem. Biol.* **17,** 135–148
37. Wang, X., Zhang, X., Dong, X. P., Samie, M., Li, X., Cheng, X., Goschka, A., Shen, D., Zhou, Y., Harlow, J., Zhu, M. X., Clapham, D. E., Ren, D., and Xu, H. (2012) TPC proteins are phosphoinositide-activated sodium-selective ion channels in endosomes and lysosomes. *Cell* **151,** 372–383
38. Cang, C., Zhou, Y., Navarro, B., Seo, Y. J., Aranda, K., Shi, L., Battaglia-Hsu, S., Nissim, I., Clapham, D. E., and Ren, D. (2013) mTOR regulates lysosomal ATP-sensitive two-pore Na^+ channels to adapt to metabolic state. *Cell* **152,** 778–790
39. Cang, C., Bekele, B., and Ren, D. (2014) The voltage-gated sodium channel TPC1 confers endolysosomal excitability. *Nat. Chem. Biol.* **10,** 463–469
40. Bakker, A. C., Webster, P., Jacob, W. A., and Andrews, N. W. (1997) Homotypic fusion between aggregated lysosomes triggered by elevated $[Ca^{2+}]_i$ in fibroblasts. *J. Cell Sci.* **110,** 2227–2238
41. Colombo, M. I., Beron, W., and Stahl, P. D. (1997) Calmodulin regulates endosome fusion. *J. Biol. Chem.* **272,** 7707–7712
42. Martinez, I., Chakrabarti, S., Hellevik, T., Morehead, J., Fowler, K., and Andrews, N. W. (2000) Synaptotagmin VII regulates Ca^{2+}-dependent exocytosis of lysosomes in fibroblasts. *J. Cell Biol.* **148,** 1141–1149
43. Vergarajauregui, S., Martina, J. A., and Puertollano, R. (2009) Identification of the penta-EF-hand protein ALG-2 as a Ca^{2+}-dependent interactor of mucolipin-1. *J. Biol. Chem.* **284,** 36357–36366
44. Li, X., Rydzewski, N., Hider, A., Zhang, X., Yang, J., Wang, W., Gao, Q., Cheng, X., and Xu, H. (2016) A molecular mechanism to regulate lysosome motility for lysosome positioning and tubulation. *Nat. Cell Biol.* **18,** 404–417
45. Yu, L., McPhee, C. K., Zheng, L., Mardones, G. A., Rong, Y., Peng, J., Mi, N., Zhao, Y., Liu, Z., Wan, F., Hailey, D. W., Oorschot, V., Klumperman, J., Baehrecke, E. H., and Lenardo, M. J. (2010) Termination of autophagy and reformation of lysosomes regulated by mTOR. *Nature* **465,** 942–946
46. Soyombo, A. A., Tjon-Kon-Sang, S., Rbaibi, Y., Bashllari, E., Bisceglia, J., Muallem, S., and Kiselyov, K. (2006) TRP-ML1 regulates lysosomal pH and acidic lysosomal lipid hydrolytic activity. *J. Biol. Chem.* **281,** 7294–7301
47. Miedel, M. T., Rbaibi, Y., Guerriero, C. J., Colletti, G., Weixel, K. M., Weisz, O. A., and Kiselyov, K. (2008) Membrane traffic and turnover in TRP-ML1-deficient cells: a revised model for mucolipidosis type IV pathogenesis. *J. Exp. Med.* **205,** 1477–1490
48. Christensen, K. A., Myers, J. T., and Swanson, J. A. (2002) pH-dependent regulation of lysosomal calcium in macrophages. *J. Cell Sci.* **115,** 599–607
49. Pryor, P. R., Reimann, F., Gribble, F. M., and Luzio, J. P. (2006) Mucolipin-1 is a lysosomal membrane protein required for intracellular lactosylceramide traffic. *Traffic* **7,** 1388–1398
50. Steinberg, B. E., Huynh, K. K., Brodovitch, A., Jabs, S., Stauber, T., Jentsch, T. J., and Grinstein, S. (2010) A cation counterflux supports lysosomal acidification. *J. Cell Biol.* **189,** 1171–1186
51. Xu, H., Delling, M., Li, L., Dong, X., and Clapham, D. E. (2007) Activating mutation in a mucolipin transient receptor potential channel leads to melanocyte loss in varitint-waddler mice. *Proc. Natl. Acad. Sci. U.S.A.* **104,** 18321–18326
52. Thompson, E. G., Schaheen, L., Dang, H., and Fares, H. (2007) Lysosomal trafficking functions of mucolipin-1 in murine macrophages. *BMC Cell Biol.* **8,** 54
53. Cerny, J., Feng, Y., Yu, A., Miyake, K., Borgonovo, B., Klumperman, J., Meldolesi, J., McNeil, P. L., and Kirchhausen, T. (2004) The small chemical vacuolin-1 inhibits Ca^{2+}-dependent lysosomal exocytosis but not cell resealing. *EMBO Reports* **5,** 883–888
54. Clarke, C. E., Benham, C. D., Bridges, A., George, A. R., and Meadows, H. J. (2000) Mutation of histidine 286 of the human P2X4 purinoceptor removes extracellular pH sensitivity. *J. Physiol.* **523,** 697–703
55. Li, R. J., Xu, J., Fu, C., Zhang, J., Zheng, Y. G., Jia, H., and Liu, J. O. (2016) Regulation of mTORC1 by lysosomal calcium and calmodulin. *eLife* **5,** e19360
56. Baars, T. L., Petri, S., Peters, C., and Mayer, A. (2007) Role of the V-ATPase in regulation of the vacuolar fission-fusion equilibrium. *Mol. Biol. Cell* **18,** 3873–3882
57. Peri, F., and Nüsslein-Volhard, C. (2008) Live imaging of neuronal degradation by microglia reveals a role for v0-ATPase a1 in phagosomal fusion *in vivo*. *Cell* **133,** 916–927
58. Zhang, X., Li, X., and Xu, H. (2012) Phosphoinositide isoforms determine compartment-specific ion channel activity. *Proc. Natl. Acad. Sci. U.S.A.* **109,** 11384–11389
59. Priel, A., and Silberberg, S. D. (2004) Mechanism of ivermectin facilitation of human P2X4 receptor channels. *J. Gen. Physiol.* **123,** 281–293

60. Lu, Y., Dong, S., Hao, B., Li, C., Zhu, K., Guo, W., Wang, Q., Cheung, K. H., Wong, C. W., Wu, W. T., Markus, H., and Yue, J. (2014) Vacuolin-1 potently and reversibly inhibits autophagosome-lysosome fusion by activating RAB5A. *Autophagy* **10,** 1895–1905
61. Huang, P., Zou, Y., Zhong, X. Z., Cao, Q., Zhao, K., Zhu, M. X., Murrell-Lagnado, R., and Dong, X. P. (2014) P2X4 forms functional ATP-activated cation channels on lysosomal membranes regulated by luminal pH. *J. Biol. Chem.* **289,** 17658–17667
62. Calcraft, P. J., Ruas, M., Pan, Z., Cheng, X., Arredouani, A., Hao, X., Tang, J., Rietdorf, K., Teboul, L., Chuang, K. T., Lin, P., Xiao, R., Wang, C., Zhu, Y., Lin, Y., *et al.* (2009) NAADP mobilizes calcium from acidic organelles through two-pore channels. *Nature* **459,** 596–600
63. Lloyd-Evans, E., Waller-Evans, H., Peterneva, K., and Platt, F. M. (2010) Endolysosomal calcium regulation and disease. *Biochem. Soc. Trans.* **38,** 1458–1464
64. Galione, A. (2015) A primer of NAADP-mediated Ca^{2+} signalling: from sea urchin eggs to mammalian cells. *Cell Calcium* **58,** 27–47
65. Brailoiu, E., Churamani, D., Cai, X., Schrlau, M. G., Brailoiu, G. C., Gao, X., Hooper, R., Boulware, M. J., Dun, N. J., Marchant, J. S., and Patel, S. (2009) Essential requirement for two-pore channel 1 in NAADP-mediated calcium signaling. *J. Cell Biol.* **186,** 201–209
66. Jha, A., Ahuja, M., Patel, S., Brailoiu, E., and Muallem, S. (2014) Convergent regulation of the lysosomal two-pore channel-2 by Mg^{2+}, NAADP, $PI(3,5)P_2$ and multiple protein kinases. *EMBO J.* **33,** 501–511
67. Patel, S., Ramakrishnan, L., Rahman, T., Hamdoun, A., Marchant, J. S., Taylor, C. W., and Brailoiu, E. (2011) The endo-lysosomal system as an NAADP-sensitive acidic Ca^{2+} store: role for the two-pore channels. *Cell Calcium* **50,** 157–167
68. Ruas, M., Davis, L. C., Chen, C. C., Morgan, A. J., Chuang, K. T., Walseth, T. F., Grimm, C., Garnham, C., Powell, T., Platt, N., Platt, F. M., Biel, M., Wahl-Schott, C., Parrington, J., and Galione, A. (2015) Expression of Ca^{2+}-permeable two-pore channels rescues NAADP signalling in TPC-deficient cells. *EMBO J.* **34,** 1743–1758
69. Schieder, M., Rötzer, K., Brüggemann, A., Biel, M., and Wahl-Schott, C. A. (2010) Characterization of two-pore channel 2 (TPCN2)-mediated Ca^{2+} currents in isolated lysosomes. *J. Biol. Chem.* **285,** 21219–21222
70. Pitt, S. J., Lam, A. K., Rietdorf, K., Galione, A., and Sitsapesan, R. (2014) Reconstituted human TPC1 is a proton-permeable ion channel and is activated by NAADP or Ca^{2+}. *Sci. Signal.* **7,** ra46
71. Pitt, S. J., Funnell, T. M., Sitsapesan, M., Venturi, E., Rietdorf, K., Ruas, M., Ganesan, A., Gosain, R., Churchill, G. C., Zhu, M. X., Parrington, J., Galione, A., and Sitsapesan, R. (2010) TPC2 is a novel NAADP-sensitive Ca^{2+} release channel, operating as a dual sensor of luminal pH and Ca^{2+}. *J. Biol. Chem.* **285,** 35039–35046
72. Cong, L., Ran, F. A., Cox, D., Lin, S., Barretto, R., Habib, N., Hsu, P. D., Wu, X., Jiang, W., Marraffini, L. A., and Zhang, F. (2013) Multiplex genome engineering using CRISPR/Cas systems. *Science* **339,** 819–823
73. Kozak, M. (1987) An analysis of 5′-noncoding sequences from 699 vertebrate messenger RNAs. *Nucleic Acids Res.* **15,** 8125–8148